Effect of Degree of Polarization on Localized Spin Density in Tightly Focusing of Vortex Beams

Zixuan Wang, Chencheng Yan, Zhen Dong, Fei Wang, Yahong Chen, and Yangjian Cai

***Abstract*—The transverse spin and orbital-to-spin angular momentum conversion during strong focusing of light beams have attracted wide interest due to the novel physics behind and their broad potential applications. In this work, we study the effect of incident beam's degree of polarization on the localized spin density of a tightly focused field. By modulating the correlation strength between two orthogonally polarized vortex modes of the incident beam, we find that the magnitude of the focal-plane transverse spin density component changes only slightly, while its spatial shape becomes an isotropic spin vortex with the decrease of the incident degree of polarization. Whereas, the longitudinal spin density, induced by the vortex phase, reduces its magnitude significantly with the decrease of incident beam's degree of polarization. The behavior of the focal-plane spin density is interpreted with the two-dimensional degrees of polarization among the tightly focused field components. Furthermore, we explore the roles of the topological charge on enhancing the longitudinal spin density for unpolarized incident beam. Our results reveal the feasibility of spin-orbit interaction with partially polarized or even completely unpolarized light, such as the thermal light.**

***Index Terms*—Degree of polarization, optical vortex, spin density, spin-orbit interaction of light, tight focusing.**

I. Introduction

ANGULAR momentum (AM) is one of the most intriguing characteristics of light [1], [2], which has played an important role in understanding the nature of light and has triggered a wide array of light applications in both classical and quantum realms [3]–[9]. The AM of light can be divided into two distinct types, i.e., the spin AM and the orbital AM. The former is related to the circular polarization of light [10], [11], i.e., with a spinning electric (and magnetic) field vector, while the intrinsic part of the orbital AM is originated from the helical wavefront (vortex phase) of a light wave [12]. In the paraxial regime of light propagation, the spin and orbital AM can be separated neatly [13] and are manifested, in the experiment during light-matter interaction, as the spinning and orbiting motions in a trapped microparticle [14], respectively.

However, in the nonparaxial regime of light propagation, such as during the tight focusing of light, the spin and orbital AM are coupled with each other, and typically, cannot be separated [15], [16]. The effect of spin-orbit coupling of light has found important roles in the directional waveguide, mode converters, and optical tweezers [15], [16]. Most spin-orbit interaction studied during light strong focusing have focused on the spin (circular polarization) control of the orbital degrees of freedom, such as spin-dependent vortex generation [17]–[20] and spin-induced beam shifts, or spin-Hall effect of light [21]–[25]. The orbit-to-spin degree of freedom, i.e., the orbitally induced spin AM in the tightly focused field, on the other hand, has received much less attention. The effects of the initial polarization state distribution and the topological charge of vortex phase on the orbitally induced spin AM in the tightly focused field have been studied numerically [26]–[32]. More recently, Zhang and coauthors proposed a principle experimental method for identifying the induced spin AM in the tightly focused beam by measuring the orientation of the major axis of the captured ellipsoidal particles in optical tweezers [33].

To the best of our knowledge, the orbit-to-spin AM conversion in the tightly focused fields considers only fully coherent and fully polarized incident beams. Thus, a natural question comes up: can the orbitally induced spin preserves when the incident beam becomes unpolarized, similar to the behavior of the transverse spin induced during strong focusing of a two-dimensional (2D) unpolarized plane wave [34]–[36]? If not, how will the degree of polarization affect the localized spin in the focal plane?

In this work, we construct a simple model for the partially polarized incident beam via a partially correlated superposition of two orthogonally polarized vortex modes and we examine the effect of incident beam's degree of polarization on the focal-plane localized spin density. We find with the decrease of the incident beam's degree of polarization, the magnitude of transverse spin component changes only slightly, whereas its spatial distribution turns from anisotropic shape to isotropic spin vortex distribution. While, the magnitude of the longitudinal spin reduces significantly with the decrease of the incident beam's degree of polarization. We also find the effect of the incident beam's topological charge on the enhancement of the

Manuscript received 6 July 2022; accepted 6 July 2022. Date of publication 11 July 2022; date of current version 18 July 2022. This work was supported in part by the National Key Research and Development Program of China under Grant 2019YFA0705000, in part by the National Natural Science Foundation of China under Grants 91750201, 11874046, 11974218, 11904247, and 12192254, and in part by the Innovation Group of Jinan under Grant 2018GXRC010. *(Corresponding authors: Yahong Chen; Yangjian Cai.)*

Zixuan Wang, Chencheng Yan, Zhen Dong, Fei Wang, and Yahong Chen are with the School of Physical Science and Technology, Soochow University, Suzhou 215006, China (e-mail: 20204208063@stu.suda.edu.cn; 20204208046@stu.suda.edu.cn; 20214008011@stu.suda.edu.cn; fwang@suda.edu.cn; yahongchen@suda.edu.cn).

Yangjian Cai is with the School of Physical Science and Technology, Soochow University, Suzhou 215006, China, and also with the Shandong Provincial Engineering and Technical Center of Light Manipulation and Shandong Provincial Key Laboratory of Optics and Photonic Devices, School of Physics and Electronics, Shandong Normal University, Jinan 250014, China (e-mail: yangjiancai@suda.edu.cn).

Digital Object Identifier 10.1109/JPHOT.2022.3189626

longitudinal spin in the unpolarized case. The evolution of the spin is interpreted well with the help of the focal-plane 2D degrees of polarization among different orthogonal field components.

II. Methods

We consider a simple model for the incident beam with controllable degree of polarization and topological charge. The incident beam is composed with well-collimated x and y orthogonally polarized Laguerre-Gaussian modes with an adjustable correlation strength, i.e., the electric fields of the beam modes are written as

$$\mathbf{E}_x(\mathbf{r}) = \mathcal{E}_x \mathrm{LG}_p^l(\mathbf{r}) \exp(\mathrm{i}k_0 z)\hat{\mathbf{e}}_x, \tag{1}$$

$$\mathbf{E}_y(\mathbf{r}) = \mathcal{E}_y \mathrm{LG}_p^l(\mathbf{r}) \exp(\mathrm{i}k_0 z)\hat{\mathbf{e}}_y, \tag{2}$$

where $\mathcal{E}_x$ and $\mathcal{E}_y$ are the random variables, k_0 is the vacuum wave number, and $\hat{\mathbf{e}}_x$ and $\hat{\mathbf{e}}_y$ are the x and y Cartesian unit vectors. The random variables satisfy that

$$\langle \mathcal{E}_x^* \mathcal{E}_x \rangle = \langle \mathcal{E}_y^* \mathcal{E}_y \rangle = 1, \tag{3}$$

$$\langle \mathcal{E}_x^* \mathcal{E}_y \rangle = \langle \mathcal{E}_y^* \mathcal{E}_x \rangle = a, \tag{4}$$

where the angle brackets and the asterisk denote the ensemble average and complex conjugate, respectively. The real factor a, bounded by $0 \le a \le 1$, controls the correlation strength between the two orthogonal beam modes. The upper and lower limits for a correspond to fully correlated and completely uncorrelated, respectively, whereas the intermediate values represent partial correlated. The deterministic part $\mathrm{LG}_p^l(\mathbf{r})$ is expressed as [12]

$$\mathrm{LG}_p^l(\mathbf{r}) = \sqrt{\frac{2p!}{\pi(p+|l|)!}} (\sqrt{2}r/w_0)^{|l|} \exp(-r^2/w_0^2) \times L_p^{|l|}(2r^2/w_0^2) \exp(\mathrm{i}l\varphi), \tag{5}$$

where $L_p^{|l|}(\cdot)$ is the generalized Laguerre polynomial with p being the radial index and l being the topological charge of vortex phase $\exp(\mathrm{i}l\varphi)$, w_0 is the waist radius, and (r, φ) are the polar coordinates.

The statistical properties of such incident beam are involved in a 2×2 cross-spectral density matrix [37], [38],

$$\mathbf{W}(\mathbf{r}_1, \mathbf{r}_2) = \langle \mathbf{E}^*(\mathbf{r}_1) \mathbf{E}^{\mathrm{T}}(\mathbf{r}_2) \rangle, \tag{6}$$

where $\mathbf{E}(\mathbf{r}) = [E_x(\mathbf{r}), E_y(\mathbf{r})]^{\mathrm{T}}$ represents the transverse electric vector of the beam taken to propagate along the z axis. The superscript T denotes the matrix transpose. The polarization matrix of the incident beam can be obtained by $\mathbf{\Phi}(\mathbf{r}) = \mathbf{W}(\mathbf{r}, \mathbf{r})$. By using (1)–(4), we obtain that

$$\mathbf{\Phi}(\mathbf{r}) = \begin{pmatrix} 1 & a \\ a & 1 \end{pmatrix} |\mathrm{LG}_p^l(\mathbf{r})|^2, \tag{7}$$

The degree of polarization of the incident beam, therefore, can be obtained as [by taking (7) into the definition of the degree of polarization in (8)] [38]

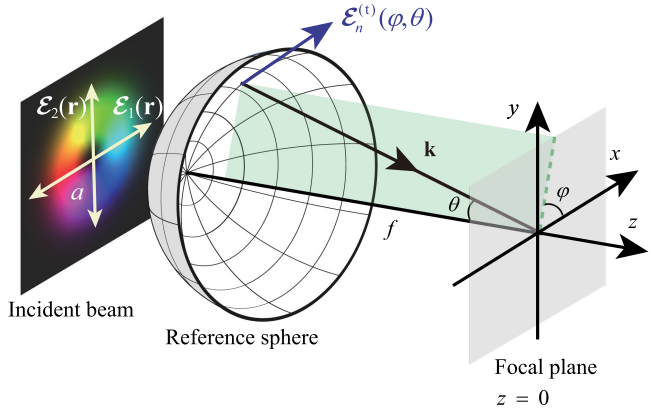

Fig. 1. Geometry related to focusing a partially polarized vortex beam by an aplanatic lens of focal length f. The incident beam is composed by the x and y polarized optical modes $\boldsymbol{\mathcal{E}}_1(\mathbf{r})$ and $\boldsymbol{\mathcal{E}}_2(\mathbf{r})$ with controllable correlation strength a. The mode vector transmitted through the lens is $\boldsymbol{\mathcal{E}}_n^{\mathrm{t}}(\varphi, \theta)$. The wavevector $\mathbf{k}$ specifies the direction of a plane wave (ray) emanating from a point on the reference sphere and is expressed in terms of angles φ and θ. The focal plane is at $z = 0$.

$$P(\mathbf{r}) = \left[2\frac{\mathrm{tr}\mathbf{\Phi}^2(\mathbf{r})}{\mathrm{tr}^2\mathbf{\Phi}(\mathbf{r})} - 1 \right]^{1/2} = a. \tag{8}$$

The degree of polarization of such incident beam is uniform in the transverse plane and is controlled by the field correlation strength a. The degree of polarization is bounded between 0 and 1 with the limits referring to fully 2D unpolarized and fully polarized beam, respectively.

The tight focusing of such partially polarized incident beam by an aplanatic object lens can be solved with the Richards–Wolf formalism. In the calculation, the incident beam is decomposed into two optical modes, i.e., $\boldsymbol{\mathcal{E}}_1(\mathbf{r})$ and $\boldsymbol{\mathcal{E}}_2(\mathbf{r})$, where $\boldsymbol{\mathcal{E}}_1(\mathbf{r}) = \mathbf{E}_x(\mathbf{r})$ and $\boldsymbol{\mathcal{E}}_2(\mathbf{r}) = \mathbf{E}_y(\mathbf{r})$. The transmission of each mode through the lens is treated within the ray picture (see Fig. 1) and the lens is taken to obey the sine condition, i.e., the incident rays are refracted at the reference sphere whose radius equals the focal distance f of the lens. The medium preceding the lens is assumed to be vacuum and the space after the lens is vacuum as well. The incident beam mode $\boldsymbol{\mathcal{E}}_n(\mathbf{r})$ with $n = (1, 2)$ propagating along the z axis is decomposed into the radially and azimuthally polarized constituents, with the related polarization unit vectors being $\hat{\mathbf{e}}_r(\mathbf{r}) = \cos\varphi\hat{\mathbf{e}}_x + \sin\varphi\hat{\mathbf{e}}_y$ and $\hat{\mathbf{e}}_\varphi(\mathbf{r}) = -\sin\varphi\hat{\mathbf{e}}_x + \cos\varphi\hat{\mathbf{e}}_y$, respectively. In the transmission, the radial polarization unit vector tilts at the off-axis points and it acquires a longitudinal component, while the azimuthal polarization unit vector remains in its original direction. The transmitted vectors can be written as $\hat{\mathbf{e}}_r^{(\mathrm{t})} = \cos\theta\hat{\mathbf{e}}_r + \sin\theta\hat{\mathbf{e}}_z$ and $\hat{\mathbf{e}}_\varphi^{(\mathrm{t})} = \hat{\mathbf{e}}_\varphi$, where θ is the angle between a ray emanating from the reference sphere and the z axis (see in Fig. 1), which is bounded between 0 and $\theta_{\max} = \arcsin(\mathrm{NA})$ with NA being the numerical aperture of the lens. The beam mode after the reference sphere, thus, becomes $\boldsymbol{\mathcal{E}}_n^{(\mathrm{t})}(\varphi, \theta) = t_r \mathcal{E}_n^{(\mathrm{rad})}(\varphi, \theta)\hat{\mathbf{e}}_r^{(\mathrm{t})} + t_\varphi \mathcal{E}_n^{(\mathrm{azi})}(\varphi, \theta)\hat{\mathbf{e}}_\varphi^{(\mathrm{t})}$, where $\mathcal{E}_n^{(\mathrm{rad})}(\varphi, \theta)$ and $\mathcal{E}_n^{(\mathrm{azi})}(\varphi, \theta)$ are the amplitudes of the radial and azimuthal components of the incident beam mode, respectively, and $t_r = t_\varphi = \sqrt{\cos\theta}$ are the transmission coefficients for the two polarization directions.

The electric field in the focal region of the tightly focused beam mode is obtained by inserting $\boldsymbol{\mathcal{E}}_n^{(\mathrm{t})}(\varphi,\theta)$ into the Richards–Wolf integral [39], i.e.,

$$\boldsymbol{\Psi}_n(\boldsymbol{\rho},z) = -\frac{\mathrm{i}f}{2\pi}\iint_{|\mathbf{k}_\perp|\le\Omega}\boldsymbol{\mathcal{E}}_n^{(\mathrm{t})}(k_x,k_y)\exp(\mathrm{i}k_z z)k_z^{-1} \times\exp[-\mathrm{i}(k_x x+k_y y)]\mathrm{d}k_x\mathrm{d}k_y, \tag{9}$$

where $\boldsymbol{\rho}=(x,y)$ denotes the transverse position vector, $\mathbf{k}_\perp=(k_x,k_y)$, and $\Omega=2\pi\mathrm{NA}/\lambda$ with λ being the wavelength. The location (φ,θ) on the reference sphere is represented in terms of the wavevector components, i.e., $k_x=-k\sin\theta\cos\varphi$, $k_y=-k\sin\theta\sin\varphi$, and $k_z=k\cos\theta$ with $k=2\pi/\lambda$. The transformation from the angles to wavevector components is made to conform to the fast numerical calculation algorithm for beam's tight focusing [40].

The 3×3 polarization matrix in the focal region can be obtained as

$$\boldsymbol{\Phi}(\boldsymbol{\rho},z)=\langle\boldsymbol{\Psi}^*(\boldsymbol{\rho},z)\boldsymbol{\Psi}^{\mathrm{T}}(\boldsymbol{\rho},z)\rangle, \tag{10}$$

where $\boldsymbol{\Psi}(\boldsymbol{\rho},z)=\boldsymbol{\Psi}_1(\boldsymbol{\rho},z)+\boldsymbol{\Psi}_2(\boldsymbol{\rho},z)$. The spin density vector [8] $\mathbf{S}(\boldsymbol{\rho},z)=\frac{\epsilon_0}{4\omega}\langle\boldsymbol{\Psi}^*(\boldsymbol{\rho},z)\times\boldsymbol{\Psi}(\boldsymbol{\rho},z)\rangle''$, with ω referring to the angular frequency, ϵ_0 representing the permittivity in vacuum, and the double prime being the imaginary part, can be extracted from the polarization matrix as

$$S_x(\boldsymbol{\rho},z)=\frac{\epsilon_0}{2\omega}\Phi''_{yz}(\boldsymbol{\rho},z), \tag{11}$$

$$S_y(\boldsymbol{\rho},z)=\frac{\epsilon_0}{2\omega}\Phi''_{zx}(\boldsymbol{\rho},z), \tag{12}$$

$$S_z(\boldsymbol{\rho},z)=\frac{\epsilon_0}{2\omega}\Phi''_{xy}(\boldsymbol{\rho},z), \tag{13}$$

where $S_x(\boldsymbol{\rho},z)$, $S_y(\boldsymbol{\rho},z)$, and $S_z(\boldsymbol{\rho},z)$ are the spin density components along the x, y, and z directions, while $\Phi_{yz}(\boldsymbol{\rho},z)$, $\Phi_{zx}(\boldsymbol{\rho},z)$, and $\Phi_{xy}(\boldsymbol{\rho},z)$ are the elements of the polarization matrix $\boldsymbol{\Phi}(\boldsymbol{\rho},z)$. The spin density components $S_x(\boldsymbol{\rho},z)$, $S_y(\boldsymbol{\rho},z)$, and $S_z(\boldsymbol{\rho},z)$ relate to the circular polarization in the yz, zx, and xy plane, respectively. The sign of the spin density components relates to the handedness of the circular polarization, i.e., the positive and negative signs correspond to the right-handed and the left-handed circular polarization states. By controlling the correlation factor a, the effect of incident beam's degree of polarization on the spin properties of a tightly focused beam can be studied conveniently.

III. Results and Discussion

In this section, we present the simulation results for the focal-plane spin density and discuss the effect of the incident beam's degree of polarization. The physics behind the results is analyzed with the help of the focal-plane 2D degrees of polarization. In the simulation, the wavelength, the beam waist, and the radial index of the incident beam are 632.8 nm, 2.5 mm, and $p=0$, respectively. The lens has a numerical aperture NA $=0.95$ and with focal length $f=3$ mm.

A. Spin Density for Linearly Polarized Beam Modes

We first examine the spin density for the (fully polarized) beam modes $\boldsymbol{\mathcal{E}}_1(\mathbf{r})$ and $\boldsymbol{\mathcal{E}}_2(\mathbf{r})$ with x and y linear initial polarization state, respectively. Fig. 2 shows the focal-plane spin density components along x, y, and z directions for the tightly focused beam modes without and with vortex phase (topological charge $l=1$). It is found that when the incident beam carries no vortex phase, the longitudinal spin density component S_z is effectively vanished [see in Fig. 2(c1) and (f1), the magnitude of S_z can be safely neglected, compared to S_x and S_y], since the transverse field components (i.e., E_x and E_y) are always in phase during strong focusing [41], and therefore, the transverse field in the xy plane is always linearly polarized.

When the vortex phase appears in the incident beam, the transverse field components E_x and E_y of the tightly focused field become out of phase in particular spatial area [27]. Thus, the circular polarization state appears as well in the transverse plane, indicating nonzero spin density along longitudinal direction [see in Fig. 2(c2) and (f2)]. In addition to the longitudinal spin density, we find x-polarized incident beam always induces the spin density dominated along y direction, i.e., S_y is dominant [see in Fig. 2(b1) and (b2)], and y-polarized incident beam always induces the spin density dominated along x direction, S_x in Fig. 2(d1) and (d2), no matter whether the incident beam carries vortex phase or not. This is because a longitudinal field component (E_z) appears during the tight focusing of a linearly polarized beam and such a longitudinal field component is out of phase of the transverse field components [41]. It is also found from Fig. 2 that before introducing the vortex phase into the incident beam, the total spin (integral over the transverse cross section) in the tightly focused beam is zero, which can be obtained from the symmetrical spatial distributions as well as the color bars from Fig. 2(a1)–(f1). When the vortex phase is introduced, we find although the transverse spin density components (S_x and S_y) are redistributed, the total transverse spin is still zero. However, it is found from the asymmetric color bars in Fig. 2(c2) and (f2) that the total longitudinal spin is not zero, indicating that the orbital AM of the incident beam induces not only the local distribution of the spin density, but also the global spin AM in the tightly focused beam.

B. Effect of Degree of Polarization

Next, we superpose the x- and y-polarized beams with different correlation strengths and study the spin density of the tightly focused superposed beams. The effect of degree of polarization of the incident beam on the focal-plane spin density distributions is examined. Fig. 3 shows the simulation results of the focal-plane spin density components along x, y, and z directions. Both the cases for the incident beam without and with vortex phase are considered in the simulation. In Fig. 3, three different superpositions are simulated, i.e., fully correlated superposition with correlation strength $a=1$, partially correlated superposition with $a=0.5$, and completely uncorrelated superposition with $a=0$, which refer to fully polarized, partially polarized, and unpolarized incident beams, respectively. We find from the simulation results that with the decrease

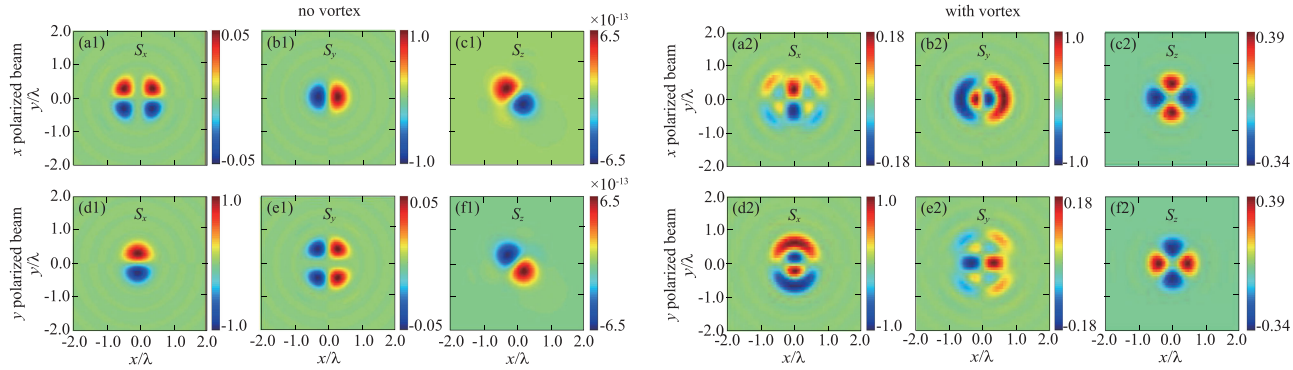

Fig. 2. Spatial distributions of the spin density components S_x, S_y, and S_z associated with the tightly focused (a1)–(c1) and (a2)–(c2) x-polarized and (d1)–(f1) and (d2)–(f2) y-polarized Laguerre-Gaussian beam at the focal plane ($z = 0$). (a1)–(f1) correspond to the incident beam with no vortex phase, while (a2)–(f2) correspond to the incident beam with vortex phase having topological charge $l = 1$. The spin distributions in the figure towards the reader.

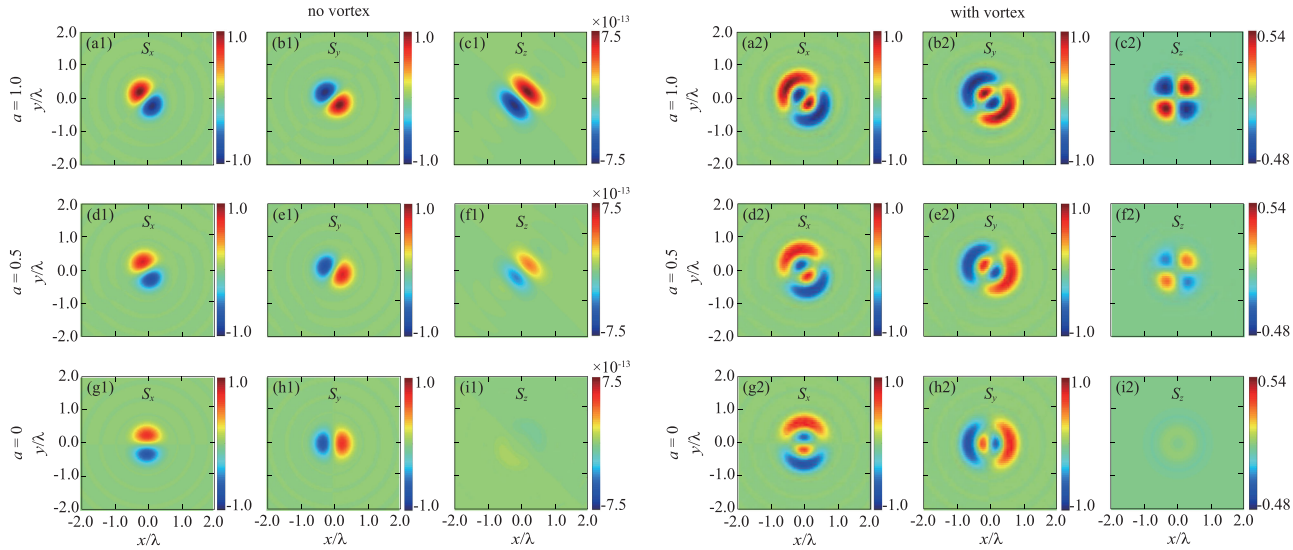

Fig. 3. Spatial distributions of the focal-plane spin density components S_x, S_y, and S_z associated with the tightly focused beams composed with x-polarized and y-polarized Laguerre-Gaussian beams with varying correlation strength: (a1)–(c1) and (a2)–(c2), $a = 1$; (d1)–(f1) and (d2)–(f2), $a = 0.5$; (g1)–(i1) and (g2)–(i2), $a = 0$. (a1)–(i1) correspond to the incident beam with no vortex phase, while (a2)–(i2) correspond to the incident beam with vortex phase having topological charge $l = 1$. The spin distributions in the figure towards the reader.

of the degree of polarization, the magnitude of the transverse spin density components (S_x and S_y) changes only slightly for both cases with and without vortex phase, although their spatial distribution rotates with the degree of polarization. For the fully polarized incident beam, both S_x and S_y are spatially distributed along -45° direction, as shown in Fig. 3(a1), (b1), and (a2), (b2), since the incident beam superposed by the x- and y-polarized modes is 45° linearly polarized. With the degree of polarization decreases, the spatial distribution for S_x rotates clockwise, while the spatial distribution for S_y rotates in a counterclockwise direction. When the degree of polarization of the incident beam vanishes, S_x and S_y are distributed orthogonally, i.e., along the y- and x-directions, respectively, indicating that a transverse spin vortex appears by tightly focusing an unpolarized light beam. The transverse spin vortex has been confirmed experimentally very recently [34]. With the introduction of the vortex phase in the incident unpolarized light beam, we find in Fig. 3(g2) and (h2) that the transverse spin vortex expands from a single ring to a double-ring with reverse spin directions.

On the other hand, the behavior of the longitudinal spin density S_z with the incident beam's degree of polarization is quite different from the transverse spin components. With the decrease of the degree of polarization, the magnitude of S_z decreases significantly. For the unpolarized incident beam ($a = 0$), the longitudinal spin density S_z is nearly vanished [Fig. 3(i2)], compared to S_x and S_y. It is noted that we only consider the longitudinal spin for the case when the incident beam carries vortex phase, since S_z is effectively vanished for the no vortex case. The spin density components for the unpolarized case can be also obtained by the incoherent superposition (algebraic sum) of the spin density components for the x- and y-polarized incident beams shown in Fig. 2. Thus, we find the spatial distributions for S_x and S_y in the unpolarized case are orthogonal to each other

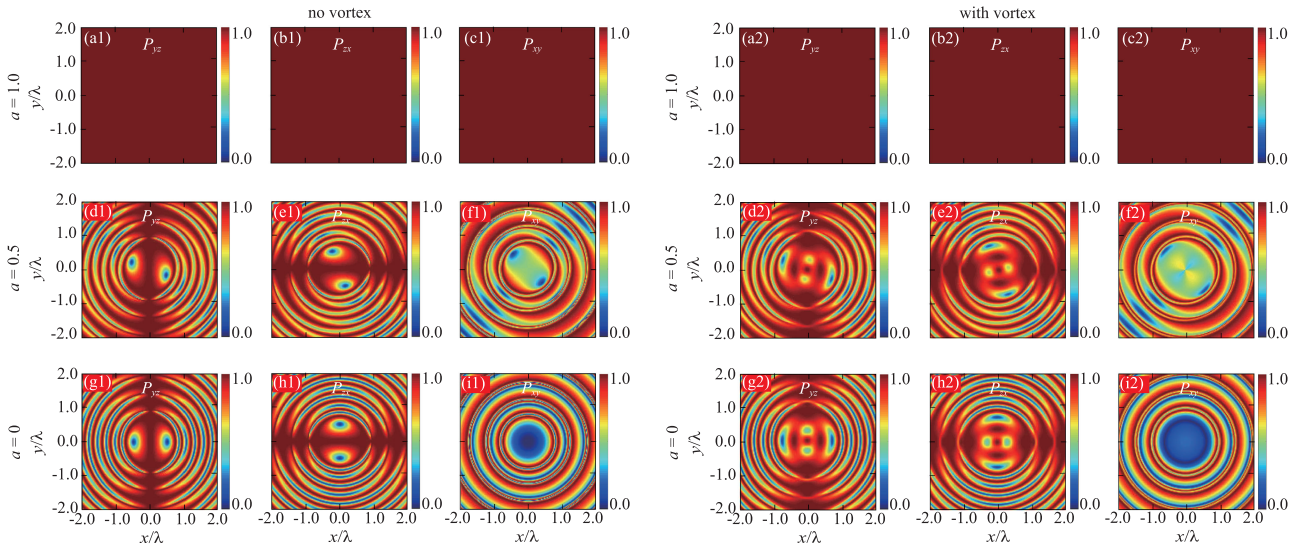

Fig. 4. Spatial distributions of the focal-plane 2D degrees of polarization P_{yz}, P_{zx}, and P_{xy} associated with the tightly focused beams composed with x-polarized and y-polarized Laguerre-Gaussian beams with varying correlation strength: (a1)–(c1) and (a2)–(c2), $a = 1$; (d1)–(f1) and (d2)–(f2), $a = 0.5$; (g1)–(i1) and (g2)–(i2), $a = 0$. (a1)–(i1) correspond to the incident beam with no vortex phase, while (a2)–(i2) correspond to the incident beam with vortex phase having topological charge $l = 1$.

and most of the magnitude in the spatial distribution of S_z is cancelled out, leading to a nearly vanished longitudinal spin for the unpolarized incident beam. For the partially polarized case, the spin density components can be viewed as the superposition of those for the fully polarized and unpolarized cases, since the incident partially polarized beam can be decomposed into fully polarized and completely unpolarized parts [38].

C. Physical Interpretation

To deeper understand the behavior of the spin density with the changes of the incident beam's degree of polarization, we now turn to study the degrees of polarization of the tightly focused beam in the focal plane. In order to explain the evolution of the spin along different orthogonal directions, we examine the 2D degrees of polarization among orthogonal field components of the tightly focused beam. The 3D degree of polarization as well as the polarization dimensionality for the tightly focused partially polarized plane wave can be found in [35], [42]. The 2D degree of polarization in the focal plane ($z = 0$) between the field components along two orthogonal directions, say α and β directions, can be obtained by

$$P_{\alpha\beta}(\boldsymbol{\rho}) = \left[2\frac{\mathrm{tr}\boldsymbol{\Phi}^2_{\alpha\beta}(\boldsymbol{\rho})}{\mathrm{tr}^2\boldsymbol{\Phi}_{\alpha\beta}(\boldsymbol{\rho})} - 1\right]^{1/2}, \tag{14}$$

where $\boldsymbol{\Phi}_{\alpha\beta}(\boldsymbol{\rho})$ denotes the 2×2 polarization matrix for the α and β field components. The matrix components can be obtained from $\boldsymbol{\Phi}(\boldsymbol{\rho}, z)$ in (10). The value of the degree of polarization $0 \le P_{\alpha\beta}(\boldsymbol{\rho}) \le 1$ reflects the strength of the correlation between the field components along α and β directions. With the decrease of $P_{\alpha\beta}(\boldsymbol{\rho})$, the field components gradually become uncorrelated. Therefore, the spin originated from the filed correlation decreases as well. The spins along x, y, and z directions are connected with the field correlations between y and z components, z and x components, and x and y components, respectively, and therefore, related to $P_{yz}(\boldsymbol{\rho})$, $P_{zx}(\boldsymbol{\rho})$, and $P_{xy}(\boldsymbol{\rho})$, respectively.

In Fig. 4, we show the simulation results for the 2D degrees of polarization for the tightly focused field in the focal plane with the incident beam having different initial degrees of polarization. Both the cases for the incident beam with and without vortex are studied. First of all, as expected that the tightly focused field in the focal plane is fully polarized when the incident beam modes are fully correlated [$a = 1$, Fig. 4(a1)–(c1) and (a2)–(c2)]. With the decrease of incident beam's degree of polarization, it is found that the tightly focused field in the focal plane becomes partially polarized or unpolarized in some areas, while the field in other areas in the focal plane is still fully polarized. The spatial distributions for the focal-plane degrees of polarization express oscillation patterns. It is noticed that within the high-spin area for S_x and S_y, the degrees of polarization $P_{yz}(\boldsymbol{\rho})$ and $P_{zx}(\boldsymbol{\rho})$ always remain the high value for the different incident beam's degrees of polarization. For instance, when the incident beam becomes unpolarized, the spatial distribution for S_x oscillates in the y direction [Fig. 3(g1)], while the spatial distribution for $P_{yz}(\boldsymbol{\rho})$ oscillates in the x direction [Fig. 4(g1)], making the high-spin area be highly polarized. The above observation indicates that the transverse field components are strongly correlated with the longitudinal field component in the focal plane no matter how uncorrelated of the incident field modes is. This is the reason why the magnitude of the transverse spin density components (S_x and S_y) changes only slightly with decreasing the incident beam's degree of polarization.

The behavior of the degree of polarization $P_{xy}(\boldsymbol{\rho})$ for the transverse field components, connected to the longitudinal spin density S_z, is quite different from $P_{yz}(\boldsymbol{\rho})$ and $P_{zx}(\boldsymbol{\rho})$. With the decrease of the incident beam's degree of polarization, $P_{xy}(\boldsymbol{\rho})$ in the high-value area of S_z decreases significantly as well. When the incident beam becomes unpolarized, it is found in Fig. 4(i1)

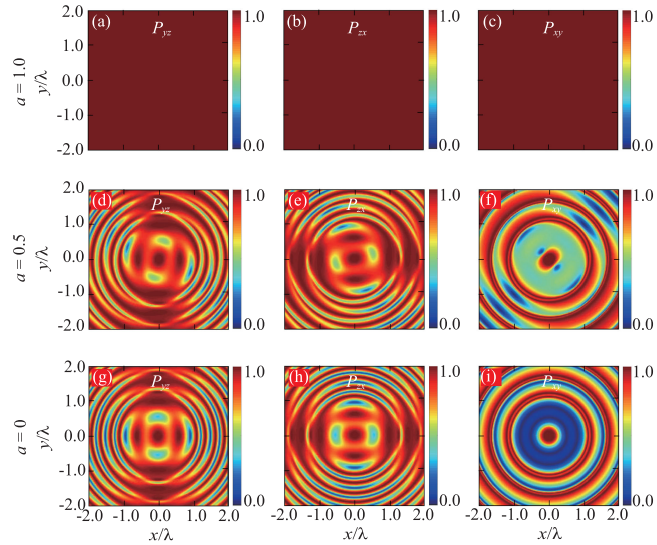

Fig. 5. Spatial distributions of the focal-plane 2D degrees of polarization P_{yz}, P_{zx}, and P_{xy} associated with the tightly focused beams composed with x-polarized and y-polarized Laguerre-Gaussian beams with varying correlation strength: (a1)–(c1) and (a2)–(c2), $a = 1$; (d1)–(f1) and (d2)–(f2), $a = 0.5$; (g1)–(i1) and (g2)–(i2), $a = 0$. The topological charge of the vortex phase in the incident beam is $l = 2$.

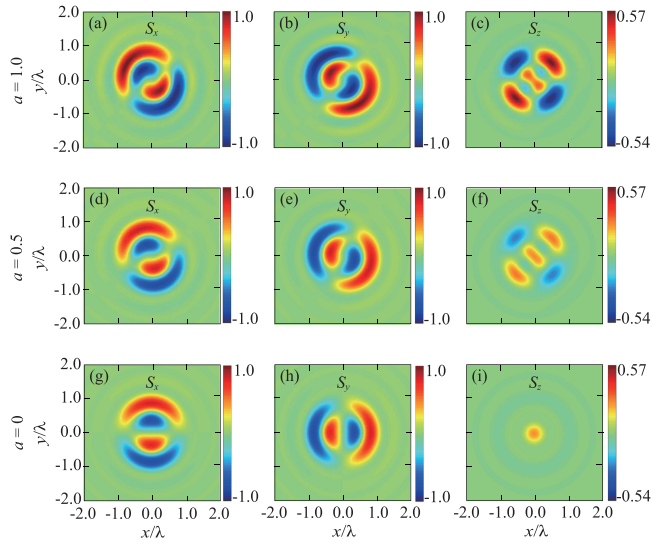

Fig. 6. Spatial distributions of the focal-plane spin density components S_x, S_y, and S_z associated with the tightly focused beams composed with x-polarized and y-polarized Laguerre-Gaussian beams with varying correlation strength: (a1)–(c1) and (a2)–(c2), $a = 1$; (d1)–(f1) and (d2)–(f2), $a = 0.5$; (g1)–(i1) and (g2)–(i2), $a = 0$. The topological charge of the vortex phase in the incident beam is $l = 2$. The spin distributions in the figure towards the reader.

and (i2) that the focal-plane degree of polarization in the high-spin area becomes effectively unpolarized, which indicates that the correlation between the focal-plane field components along x and y directions is very weak. Therefore, the magnitude of the longitudinal spin density S_z decreases with reducing the incident beam's degree of polarization. In addition to the magnitude of the degree of polarization, we find that with the decrease of the incident beam's degree of polarization, the spatial distribution for $P_{xy}(\boldsymbol{\rho})$ gradually becomes isotropic, while $P_{yz}(\boldsymbol{\rho})$ and $P_{zx}(\boldsymbol{\rho})$ still show the anisotropic spatial distribution, indicating that the isotropic property in the x and y field components of an unpolarized incident beam maintains during strong focusing.

D. *Effect of Topological Charge*

In Fig. 4(i1) and (i2), we find that by introducing the vortex phase (with topological charge $l = 1$) in the incident beam's wavefront, the magnitude of $P_{xy}(\boldsymbol{\rho})$ in the central area increases. We now increase the topological charge from $l = 1$ to $l = 2$ and study the effect of topological charge on the focal-plane 2D degrees of polarization and spin density distributions. Fig. 5 displays the spatial distribution of the focal-plane 2D degrees of polarization among different field components for the incident beams with different degrees of polarization and with topological charge $l = 2$. Fig. 6 shows the corresponding focal-plane spin density components. It is found from Fig. 5 that the spatial distributions for $P_{yz}(\boldsymbol{\rho})$ and $P_{zx}(\boldsymbol{\rho})$ change only slightly, i.e., the distributions expand a bit with the increase of the topological charge. Thus, as shown in Fig. 6 the spatial distributions for S_x and S_y expand as well with l increasing. However, the spatial distributions of $P_{xy}(\boldsymbol{\rho})$ and S_z have the different behavior with the increase of the incident beam's topological charge. We find $P_{xy}(\boldsymbol{\rho})$ in the central area always maintains the high value with the decrease of the incident beam's degree of polarization, which means that the field components along x and y directions are highly correlated in the focal plane although they are completely uncorrelated at the source. Due to such counterintuitive degree of polarization in the focal plane, we find in Fig. 6 that the magnitude of the focal-plane longitudinal spin density S_z is enhanced significantly for the unpolarized incident beam. Compared to the spatial distribution of S_z shown in Fig. 3(i2), we find S_z becomes a bright spot from a dark ring distribution with the topological charge increased from 1 to 2. The difference is induced by the changes of the correlation among the field components along x and y directions [see in Figs. 4(i2) and 5(i)]. The topological charge provides a novel degree of freedom to govern the spin density distribution for a tightly focused unpolarized light.

IV. Conclusion

In summary, we have examined the effect of the incident beam's degree of polarization on the focal-plane local spin density distribution of the tightly focused light beam. We adopted a simply model for the incident beam having controllable, spatially uniform degree of polarization. The incident beam is composed by two orthogonally polarized (x and y polarized) Laguerre-Gaussian vortex modes with an adjustable correlation strength that controls the incident beam's degree of polarization. Our results showed that with the decrease of the incident beam's degree of polarization, the magnitude for the focal-plane transverse spin component changes only slightly, while its spatial distribution gradually changes from the anisotropic shape to the isotropic spin vortex distribution. With the introduction of the vortex phase (with topological charge $l = 1$) in the incident beam, we found that the focal-plane spin vortex expands from a single ring to a double-ring distribution. On the other hand,

it is found that with the decrease of the incident beam's degree of polarization, the longitudinal spin density, induced by the vortex phase of the incident beam, changes its magnitude significantly. When the incident beam becomes completely unpolarized, the focal-plane longitudinal spin density for the case when $l = 1$ is nearly vanished. It is noted that we only consider the homogeneous polarization state for the incident beam. The inhomogeneous vectorial polarization of incident beam will induce the changes of spin density in the focal plane. However, the effect of degree of polarization (describing the correlation strength between the orthogonal field components at a single spatial point) on the focal-plane spin density will not change with the switch of the incident beam's initial polarization state, i.e., the longitudinal spin always decreases with decreasing the incident beam's degree of polarization.

The evolution properties of the focal-plane spin density have been interpreted with the help of the two-dimensional degrees of polarization among any two of the three orthogonal components of the tightly focused field, since the two-dimensional degrees of polarization describe the correlation strength between orthogonal field components, which is the origin of the spin angular momentum. We found that in the high-spin area, the focal-plane degrees of polarization among y and z field components, as well as among z and x field components always remain the high value, whereas the focal-plane degree of polarization among x and y field components reduces largely with the decrease of the incident beam's degree of polarization. However, it is found that with the topological charge increasing from $l = 1$ to $l = 2$, the x and y field components in the central area of the focal plane become highly correlated even though they are completely uncorrelated in the source plane, which explains the enhancement of the longitudinal spin density in the unpolarized case with the increase of the incident beam's topological charge. We expect the findings in this work can find uses in the studies of spin-orbit interaction with unpolarized light, such as natural light and blackbody radiation [43], [44]. As a final remark, the localized spin density vector of a tightly focused partially polarized vortex beam can be probed with the help of a near-field optical microscope by placing a nanoscatterer in the focal area. The scattered light, which can be measured in the far field, carries all the polarization information about the tightly focused light in the near field [34], [45]. We expect that the technique of photo-induced force microscopy [46], [47] can be used to further increase the signal to noise ratio and the resolution of the near-field polarization information.

REFERENCES

[1] L. Allen, S. M. Barnett, and M. J. Padgett, *Optical Angular Momentum*. Bristol, U.K.: IOP Publishing, 2003.

[2] D. L. Andrews and B. Mohamed, Eds. *The Angular Momentum of Light*. Cambridge, U.K.: Cambridge Univ. Press, 2012.

[3] D. G. Grier, "A revolution in optical manipulation," *Nature*, vol. 424, no. 6950, pp. 810–816, 2003.

[4] X. Fang *et al.*, "Nanophotonic manipulation of optical angular momentum for high-dimensional information optics," *Adv. Opt. Photon.*, vol. 13, no. 4, pp. 772–833, 2021.

[5] A. E. Willner, K. Pang, H. Song, K. Zou, and H. Zhou, "Orbital angular momentum of light for communications," *Appl. Phys. Rev.*, vol. 8, no. 4, 2021, Art. no. 041312.

[6] J. Ni *et al.*, "Multidimensional phase singularities in nanophotonics," *Science*, vol. 374, no. 6566, 2021, Art. no. eabj0039.

[7] P. Shi, L. Du, and X. Yuan, "Spin photonics: From transverse spin to photonic skyrmions," *Nanophotonics*, vol. 10, no. 16, pp. 3927–3943, 2021.

[8] J. Chen, C. Wan, and Q. Zhan, "Engineering photonic angular momentum with structured light: A review," *Adv. Photon.*, vol. 3, no. 6, 2021, Art. no. 064001.

[9] A. S. Solntsev, G. S. Agarwal, and Y. S. Kivshar, "Metasurfaces for quantum photonics," *Nature. Photon.*, vol. 15, no. 5, pp. 327–336, 2021.

[10] J. H. Poynting, "The wave-motion of a revolving shaft, and a suggestion as to the angular momentum in a beam of circularly-polarized light," *Proc. Roy. Soc. London Ser. A, Containing Papers Math. Phys. Character*, vol. 82, no. 557, pp. 560–567, 1909.

[11] R. A. Beth, "Mechanical detection and measurement of the angular momentum of light," *Phys. Rev.*, vol. 50, no. 2, pp. 115–125, 1936.

[12] L. Allen, M. W. Beijersbergen, R. J. C. Spreeuw, and J. P. Woerdman, "Orbital angular-momentum of light and the transformation of Laguerre-Gaussian laser modes," *Phys. Rev. A*, vol. 45, no. 11, pp. 8185–8189, 1992.

[13] M. V. Berry, "Paraxial beams of spinning light," in *Singular Optics*, Philadelphia, PA, USA: SPIE, 1998, pp. 6–11.

[14] V. Garcés-Chávez, D. McGloin, M. J. Padgett, W. Dultz, H. Schmitzer, and K. Dholakia, "Observation of the transfer of the local angular momentum density of a multiringed light beam to an optically trapped particle," *Phys. Rev. Lett.*, vol. 91, no. 9, 2003, Art. no. 093602.

[15] K. Y. Bliokh, F. J. Rodríguez-Fortuño, F. Nori, and A. V. Zayats, "Spin-orbit interactions of light," *Nature Photon.*, vol. 9, no. 12, pp. 156–163, 2015.

[16] A. Aiello, P. Banzer, M. Neugebauer, and G. Leuchs, "From transverse angular momentum to photonic wheels," *Nature Photon.*, vol. 9, no. 12, pp. 789–795, 2015.

[17] Y. Zhao, J. S. Edgar, G. D. M. Jeffries, D. McGloin, and D. T. Chiu, "Spin-to-orbital angular momentum conversion in a strongly focused optical beam," *Phys. Rev. Lett.*, vol. 99, no. 7, 2007, Art. no. 073901.

[18] K. Y. Bliokh, M. A. Alonso, E. A. Ostrovskaya, and A. Aiello, "Angular momenta and spin-orbit interaction of nonparaxial light in free space," *Phys. Rev. A*, vol. 82, no. 6, 2010, Art. no. 063825.

[19] K. Y. Bliokh *et al.*, "Spin-to-orbital angular momentum conversion in focusing, scattering, and imaging systems," *Opt. Exp.*, vol. 19, no. 27, pp. 26132–26149, 2011.

[20] V. V. Kotlyar, A. G. Nalimov, A. A. Kovalev, A. P. Porfirev, and S. S. Stafeev, "Spin-orbit and orbit-spin conversion in the sharp focus of laser light: Theory and experiment," *Phys. Rev. A*, vol. 102, no. 3, 2020, Art. no. 033502.

[21] M. Neugebauer *et al.*, "Geometric spin hall effect of light in tightly focused polarization-tailored light beams," *Phys. Rev. A*, vol. 89, no. 1, 2014, Art. no. 013840.

[22] X. Ling *et al.*, "Realization of tunable spin-dependent splitting in intrinsic photonic spin Hall effect," *Appl. Phys. Lett.*, vol. 105, no. 15, 2014, Art. no. 151101.

[23] X. Ling *et al.*, "Recent advances in the spin hall effect of light," *Rep. Prog. Phys.*, vol. 80, no. 6, 2017, Art. no. 066401.

[24] W. Shu *et al.*, "Three-dimensional spin hall effect of light in tight focusing," *Phys. Rev. A*, vol. 101, no. 2, 2020, Art. no. 023819.

[25] H. Li, C. Ma, J. Wang, M. Tang, and X. Li, "Spin-orbit Hall effect in the tight focusing of a radially polarized vortex beam," *Opt. Exp.*, vol. 29, no. 24, pp. 39419–39427, 2021.

[26] M. Li *et al.*, "Orbit-induced localized spin angular momentum in strong focusing of optical vectorial vortex beams," *Phys. Rev. A*, vol. 97, no. 5, 2018, Art. no. 053842.

[27] P. Yu *et al.*, "Orbit-induced localized spin angular momentum in the tight focusing of linearly polarized vortex beams," *Opt. Lett.*, vol. 43, no. 22, pp. 5677–5680, 2018.

[28] P. Meng, Z. Man, A. P. Konijnenberg, and H. P. Urbach, "Angular momentum properties of hybrid cylindrical vector vortex beams in tightly focused optical systems," *Opt. Exp.*, vol. 27, no. 24, pp. 35336–35348, 2019.

[29] Z. Man, X. Dou, and H. P. Urbach, "The evolutions of spin density and energy flux of strongly focused standard full Poincaré beams," *Opt. Commun.*, vol. 458, 2020, Art. no. 124790.

[30] T. Geng, M. Li, and H. Guo, "Orbit-induced localized spin angular momentum of vector circular airy vortex beam in the paraxial regime," *Opt. Exp.*, vol. 29, no. 9, pp. 14069–14077, 2021.

[31] V. V. Kotlyar, A. G. Nalimov, S. S. Stafeev, A. A. Kovalev, and A. P. Porfirev, "Orbital energy and spin flows in a strong focus of laser light," *IEEE Photon. J.*, vol. 12, no. 5, 2020, Art. no. 4501713.

[32] X. Pang, H. Zhang, M. Hu, and X. Zhao, "Constructing spin density vector twists with spin density singularity," *IEEE Photon. J.*, vol. 14, no. 3, 2022, Art. no. 6523508.
[33] X. Zhang *et al.*, "Understanding of transverse spin angular momentum in tightly focused linearly polarized vortex beams," *Opt. Exp.*, vol. 30, no. 4, pp. 5121–5130, 2022.
[34] J. S. Eismann *et al.*, "Transverse spinning of unpolarized light," *Nature Photon.*, vol. 15, no. 2, pp. 156–161, 2021.
[35] Y. Chen *et al.*, "Structure of transverse spin in focused random light," *Phys. Rev. A*, vol. 104, no. 1, 2021, Art. no. 013516.
[36] K. A. Forbes, "Optical helicity of unpolarized light," *Phys. Rev. A*, vol. 105, no. 2, 2022, Art. no. 023524.
[37] L. Mandel and E. Wolf, *Optical Coherence and Quantum Optics*. Cambridge, U.K.: Cambridge Univ. Press, 1995.
[38] A. T. Friberg and T. Setälä, "Electromagnetic theory of optical coherence," *J. Opt. Soc. Amer. A*, vol. 33, no. 12, pp. 2431–2442, 2016.
[39] M. Leutenegger, R. Rao, A. Leitgeb, and T. Lasser, "Fast focus field calculations," *Opt. Exp.*, vol. 14, no. 23, pp. 11277–11291, 2006.
[40] R. Tong *et al.*, "Fast calculation of tightly focused random electromagnetic beams: Controlling the focal field by spatial coherence," *Opt. Exp.*, vol. 28, no. 7, pp. 9713–9727, 2020.
[41] M. Neugebauer, T. Bauer, A. Aiello, and P. Banzer, "Measuring the transverse spin density of light," *Phys. Rev. Lett.*, vol. 114, no. 6, 2015, Art. no. 063901.
[42] Y. Chen *et al.*, "Polarimetric dimension and nonregularity of tightly focused light beams," *Phys. Rev. A*, vol. 101, no. 5, 2020, Art. no. 053825.
[43] S. Divitt and L. Novotny, "Spatial coherence of sunlight and its implications for light management in photovoltaics," *Optica*, vol. 2, no. 2, pp. 95–103, 2015.
[44] K. Blomstedt, A. T. Friberg, and T. Setälä, "Classical coherence of blackbody radiation," *Prog. Opt.*, vol. 62, pp. 293–346, 2017.
[45] K. Lindfors, A. Priimagi, T. Setälä, A. Shevchenko, A. T. Friberg, and M. Kaivola, "Local polarization of tightly focused unpolarized light," *Nature Photon.*, vol. 1, no. 4, pp. 228–231, 2007.
[46] J. Zeng *et al.*, "Sharply focused azimuthally polarized beams with magnetic dominance: Near-field characterization at nanoscale by photoinduced force microscopy," *ACS Photon.*, vol. 5, no. 2, pp. 390–397, 2018.
[47] J. Zeng *et al.*, "Exclusive magnetic excitation enabled by structured light illumination in a nanoscale MIE resonator," *ACS Nano*, vol. 12, no. 9, pp. 12159–12168, 2018.